

Superposed Strokes Analysis by Conoscopic Holography as aid for Handwriting Expert

Giuseppe SCHIRRIPA SPAGNOLO, Carla SIMONETTI, Lorenzo COZZELLA

INFM - Dipartimento di Ingegneria Elettronica, Università degli Studi "Roma Tre"

Via della Vasca Navale 84, 00146 Roma (Italy)

Abstract

On the basis of the Legal issue there is the problematic of validate signature as well as handwritten documents. A helpful method in this sense is the so-called Superposed Strokes Analysis, based on the observation of some characteristics in the writing, such as some letters and their dynamic.

This paper introduces a new promising technique for the Superposed Strokes Analysis based on the Conoscopic Holography. Through a non-contact three-dimensional measure is created a 3D profile of the superposed strokes that allow a more suitable analysis based on particular writing characteristics.

In conclusion, we propose an opto-electronic application, integrated with multimedia techniques, in order to improve the Graphology Analysis during Legal issues.

Keywords: 3D digitizing, conoscopic holography, Graphology, superposed strokes analysis.

1. Introduction

The Legal Graphology requests, apart from a psychological, also objective analysis to aid the handwriting experts for their determinations [1,2].

The necessity of using a non-invasive and non-destructive approaches, for avoiding to damage the document, have requested the introduction of new techniques that provide both aid to handwriting expert for a more accurate opinion about handwritten documents and the conservation of documents itself.

Among the most spread-counterfeited technique, the simplest and more banal is the trace one. But the more expert counterfeiters use the so-called “Freehand Technique”. This consists of an exercise of reproduction on the more characteristics points of the original document handwriting.

The handwriting of a person indicates his personality; handwriting experts give particular attention to those letters that characterize a handwritten document, like: d, h, l, t, g, p, q.

All these letters having the characteristic to have frequent crossing of ascending and descending strokes.

For each letter is used a dedicated analytic study. In fact, if the letter is excessively stretched out respect to its central body, can be deduced by that a particular writer’s psychological profile and, consequently the handwriting expert can write out a first personality sketch.

Similarly an analysis could be performed on letters like f and t, in which the slop of the horizontal dash corresponds to a different personality deformation.

In relation to the above considerations, in this work the analysis of strokes in a handwritten document is centered on some physical points:

- Pressure made during the writing (including its variations)
- The dynamic of the document drafting.

The counterfeiter will be not able to reproduce the pressure normally used by the original writer during the document drafting and, after time, thanks to the “Paper Hysteresis” analysis, could be possible highlight the existing discrepancies between the counterfeit document Hysteresis cycle and the original document one.

Analysis covers also the handwritten dynamic characteristics; in fact the writing techniques of some letters could be different, creating some crossing, among ascending and descending strokes, more smooth or angular.

Can be defined two kind of writing, depending on different pressure:

- **SQUATTY WRITING OF FIRST TYPE:** writing in which ascending strokes are more marked than descending ones, because the hand loads the energy in the realization of the ascending stroke, and then unload it during the descending one, for increasing the pressure used to draw the stroke.
- **SQUATTY WRITING OF SECOND TYPE:** writing characterized by mirco-stoppings in the gesture that create small ink stagnation on the paper and that denotes the person emotionalism.

With the help of an electro-optic system it is possible acquiring, under cloud of points, an area in which there is a strokes superposing. Obtained the writing profile, it is possible provides the strokes depth and consequently the crossing dynamic.

This work propose a new 3D acquisition and digitalizing techniques technique, based on Conoscopic Holography⁶ for implementing in a semi-automatic way the above-described analysis,

providing a valid and useful support to the Graphology experts for identifying the truthfulness of signatures and handwritten documents.

In this work has also been introduced the Paper Hysteresis problematic and its effects on the described Analysis.

Information about the shape of a set of strokes (i.e. a signature) is acquired in a no-contact way, using the state of the art of optical profilometry methods.

2. Conoscopic holography

Generally speaking, because of conservation necessity, the digitalization of a set of strokes made on a handwritten document could be made in a conservation site. For this reason, the 3D digitalization system must be compact and rugged for easy transportation and rapid set-up. Furthermore, the optic sensor must be immune to ambient light conditions. Finally, technical issues such as security of equipment, personnel, and handwritten document being measured also require attention.

When working in the field, we must worry not only about hardware failure but also about the possibility of progressive and unnoticed degradations in performance caused, for example, by equipment damage or changing environmental conditions. Hence, in addition to robust sensors design, regular on-site validation of sensor performance becomes an essential task, especially under fluctuating conditions.

A Conoscopic range finder (based on Conoscopic holography) is well suited to provide accurate 3D profile of handwritten documents. At present, cheap Conoscopic systems, well adapted to work in field, are available.

Conoscopic holography has already been described in depth many times [3-5], here we present only what is necessary to understand the following discussion.

Conoscopic holography is a simple implementation of a particular type of polarized light interference process, which uses a birefringent crystal.

In ordinary holography, each object point is interferometrically recorded as a Fresnel zone plate (FZP). The interference pattern is formed between an object beam and a reference beam using a coherent light source. The object and reference beams propagate with the same velocity, but follow different geometrical paths.

In Conoscopic holography, the object and reference beams of coherent holography are replaced by the ordinary and the extraordinary components of a single beam propagating in birefringent media. Therefore, the signal and reference beams have the same geometrical paths but different optical path-lengths; the two beams are naturally coherent one with the other and therefore the technique allows to produce holograms, even with non coherent light.

Conoscopic holography has some advantages over classical holography if spatially limited illuminated area is concerned (one singular point):

- much greater stability than classical holography because the geometrical paths of both wave fronts are almost the same;
- an interfringe distance adjustable to common CCD camera resolution; thus interfacing with a computer system is facilitated;
- the possibility of using not spatially coherent quasi-monochromatic light because of the small phase difference, which is introduced.

The basic principle resides in considering a crystal sandwiched between two circular polarizers in order to provide an interference pattern (see Figure 1).

Each object point $P(x, y, z)$ either emits, diffuses or reflects quasi-monochromatic, non-polarized and spatial incoherent light intensity $I(P)$. A ray, with wavelength λ , making an angle α with the system optical axis (see Figure 2) passes through the first circular polarizer, which generates two orthogonal polarized, 90° phase shifted, rays. Within the uniaxial (birefringent) crystal, the two rays propagate according to two modes, namely the ordinary and the extraordinary mode, with different velocities.

The wave velocity in a medium depends on the refractive index. In uniaxial crystals, the ordinary refractive index is constant, while the extraordinary index depends on the angle between the ray and the crystal optical axis, and therefore on the object's point location. If the ordinary and the extraordinary indices of refraction are n_0 and n_E , respectively, and their difference is $\Delta n = (n_0 - n_E)$, then two orthogonal polarized waves will propagate, one with an index of refraction n_0 (ordinary ray), and the second, the extraordinary ray, with an index of refraction $n_E(\alpha)$ given approximately by [6]

$$n_E(\alpha) \approx n_0 + \Delta n \sin^2 \alpha \quad (1)$$

where $\Delta n = (n_0 - n_E)$.

The retardation angle, or the difference of optical path between extraordinary and ordinary waves, is given by

$$\Delta\varphi = \frac{2\pi}{\lambda} \cdot \frac{L}{\cos\alpha} \Delta n \sin^2 \alpha \quad \text{if } \alpha \text{ is small} \quad \Rightarrow \quad \Delta\varphi \approx \frac{2\pi}{\lambda} \cdot L \Delta n \alpha^2. \quad (2)$$

For simplicity, we use the convention that the light outside the crystal propagates in a medium of refractive index n_0 .

The intensity at $R(x', y', 0)$ on the recording plane ($z = 0$) due to point source $P(x, y, z)$ will be given by (see Figure 2)

$$I(R, P) = I(P) \left\{ 0.5 + 0.5 \cos [\Delta\phi(P, R)] \right\}. \quad (3)$$

The total intensity $I(R)$ recorded at point R is given by

$$I(R) = \int_s I(R, P) dP = \int_s I(P) T(R, P) dP \quad (4)$$

where s contains all the points P in the illuminated object surface from which light can reach R and $T(R, P)$ is the impulse response of the system. Using Eq. (2) and paraxial approximation

$$\left[\alpha^2 \approx \left[(x - x')^2 + (y - y')^2 \right] / z^2 \right] \quad (5)$$

we obtain

$$\left[I(R, P) = I(P) T(R, P) = I(P) \left\{ 0.5 + 0.5 \cos \left\{ \frac{2\pi L \Delta n}{z^2 \lambda} \left[(x - x')^2 + (y - y')^2 \right] \right\} \right\} \right]. \quad (6)$$

Equation (6) represents a Fresnel zone plate (FZP) centered at $[x' = x, y' = y]$, plus a constant bias.

We note that the distance z (the depth coordinate) acts as a parameter, which changes the fringe spacing.

The number of fringes (N_F) in the Fresnel zone plate is:

$$\left[\Delta\phi = 2\pi N_F \Rightarrow N_F \approx \frac{L \Delta n \alpha^2}{\lambda} \approx \frac{L \Delta n A^2}{\lambda z_0^2} \Rightarrow z_0 = \sqrt{\frac{N_F \lambda}{L \Delta n A^2}} \right], \quad (7)$$

where $2A$ is the size of the FZP and z_0 is the mean distance from the illuminated surface of the object to the recording plane.

By Eq. (7), depth estimation is possible by illuminating a very small area (by a focalized laser beam) and counting the fringe number N_F . Obviously, for continuous depth estimation, a calibration curve $z_0(N_F)$ is needed. This curve yields the distance z_0 from the object surface to the hologram center as a function of fringe number N_F . At fractional N_F , depth estimation is achieved by using polynomial interpolation.

3. The conoscopic range finder

For the application proposed in this paper, we have used a commercially available Conoscopic range finder made by Optimet [7]. The set up is shown in Figure 3.

In particular, the system consists of:

- A laser diode used as quasi-monochromatic light source. The light emitted by the diode impinges on a cube beam-splitter to realize collinearity between projected laser beam and view axis. This on-axis configuration avoids the problem of the shades, present in all system based on optical triangulation.
- A conoscopic head as previously described.
- A control and digital processing box. The control box counts the fringes, which are detected and imaged by sensitive area of the CCD detector. Furthermore, it performs all the digital processing

required and outputs the distance data. The system also provides an indication of the measurement precision, allowing bad data points to be eliminated.

- A personal computer (PC). The PC manages the overall measurement process.

This type of conoscopic range finder is a very versatile system, which can work with sub-micron resolution.

The system, used in this work is in the fix-probe configuration. The fix-probe configuration consists in keeping the conoscopic probe fixed and placing the object to be analyzed on a precise micrometric x - y table. This configuration is suitable for analyzing small objects like tiny strokes on ancient handwritten documents.

4. Processing to analyze superposed strokes by a 3D model

The utilization of conoscopic range finder and related 3D reconstruction has permitted to analyze the strokes superposition deciding in an objective way the interest area around the strokes intersection point.

For properly managing the sample scanning, it could be possible to define in a precision way the application point, the scanning area and the sampling step so as to acquire the image points.

After having completed the sampling scanning, the analysis is performed by reconstructing, in three-dimensional way, the sample image by a dedicated 3D reconstruction software.

Observing the reconstructed 3D image, strokes appears like furrow, but for recognize the crossing dynamic the observer shall put attention on some particular characteristics.

A first activity to perform is to verify the presence of some “bumps”, fitfulness generated by paper due to the writer’s pressure, left from the second strokes that crosses upon the first one.

The presence of these irregularities is localized in the strokes crossing zone, along the first handwritten stroke line and have to stand out against paper depression created by the double pen passage.

The strokes and bumps visibility is due to the kind of paper on which we have written and to the kind of pen that we have used for carrying out them.

Among the numerous analyzed samples we have noted that fountain pens or papers particularly bright don’t bring to any significant results. In Figures 4 and 5 are reported two typical examples of analysis, which allow to confirm the dynamic of the strokes crossing.

In Figure 4(a) and 4(b) is shown the crossing zone from two different angles for highlighting the presence of bumps along the first (F) stroke direction, as indicating in Figure 4(b). Figure 4(c) is the reverse along z-axis image that clearly shows that the second (S) stroke was made after the stroke F, because its shape is continuous, whereas the F stroke one is interrupted. As can be noted, a characteristic of the second strokes is that it “cuts” the first one. Using this assertion is easier to reconstruct the crossing dynamic.

A second verification is shown in Figure 5.

5. Conclusion

The following tables report, in a synthetic way, the results that we have obtained during all the performed scanning. All these results are divided in three different tables.

The $n1/n2$ ratio, reported in all the tables, indicates the ratio between the scanning from which it could be possible clearly identifying the strokes superposing order ($n1$) in relation with all the scanning performed ($n2$).

The Table 1 summarizes the results obtained in relation with the kind of paper and pens used on that.

The Table 2 shows all the obtained results in relation only with the paper used.

Finally, the Table 3 shows the results in relation only with the kind of pen.

REFERENCES

1. P.R.S. Foli, *Handwriting as an Index to Character*, Pearson Ltd, London 1902.
2. N. Bradley, *Graphology Digest Factbook*, 1999.
3. G. Y. Sirat and D. Psaltis, "Conoscopic holography", *Opt. Lett.*, **10**, pp. 4-6, 1985.
4. G. Y. Sirat and D. Psaltis, "Conoscopic Holograms", *Opt. Comm.* **65** , pp. 243- 249, 1988.
5. Y. Malet and G. Y. Sirat, "Conoscopic Holography application: multipurpose rangefinders", *J. Opt.* **29** , pp. 183-187 , 1998.
6. M. Born and E. Wolf, *Principles of Optics*, New York: Pergamon, 1975
7. OPTIMET – Optical Metrology Ltd., <http://www.optimet.com>.

FIGURE CAPTIONS

Figure 1 – Conoscopic principle.

Figure 2 – Propagation of light in a uniaxial crystal.

Figure 3 – Basic Conoscopic range finder setup.

Figure 4 – First profilometric acquisition by means of Conoscopic holography. This strokes are made by Felt pen on Thin Cardboard. (a) 3D viewer of the strokes profile. It is possible to note the regularity in the line S. (b) 3D viewer of the strokes profile. it is possible to note the presence of the bumps. (c) 3D viewer with mirror in z-axis.

Figure 5 – First profilometric acquisition by means of Conoscopic holography. This strokes are made by BIC pen on Common Paper. (a) 3D viewer of the strokes profile. It is possible to note the regularity in the line S. (b) 3D viewer of the strokes profile. it is possible to note the presence of the bumps. (c) 3D viewer with mirror in z-axis.

TABLE CAPTIONS

Table I – Synthesis of Results (success recognition / total experiments).

Table II – Synthesis of results obtained for each kind of paper (success recognition / performed experiments).

Table III - Synthesis of results obtained for each kind of pen (success recognition / performed experiments).

TABLE I

	BIC Pen	Ballpoint Pen with fine point	Fountain Pen	Liquid Ink Pen	Felt Pen	Felt Pen with fine point	Carbon Paper
Common Paper	16/16	9/9	9/12	1/1	2/2	8/8	7/9
Thin Cardboard	6/6	3/4	0/2	1/1	2/2	6/6	2/3
Flimsy Paper	2/2	2/2	1/1	1/1	1/1	1/3	
Tracing Paper	2/2	2/2	0/1	1/1	1/1	2/3	1/1
Official Stamped Paper	2/2	3/3	1/1	1/1	0/1	3/3	1/1
Cheque Paper	3/3	2/2	1/1	1/1	0/1	3/3	1/1

TABLE II

Common Paper	52/57
Thin Cardboard	20/24
Flimsy Paper	9/10
Tracing Paper	9/11
Official Stamped Paper	11/12
Cheque Paper	11/12

TABLE III

BIC Pen	31/31
Ballpoint Pen with fine point	21/22
Fountain Pen	12/18
Liquid Ink Pen	6/6
Felt Pen	6/8
Felt Pen with fine point	23/26
Carbon Paper	12/15

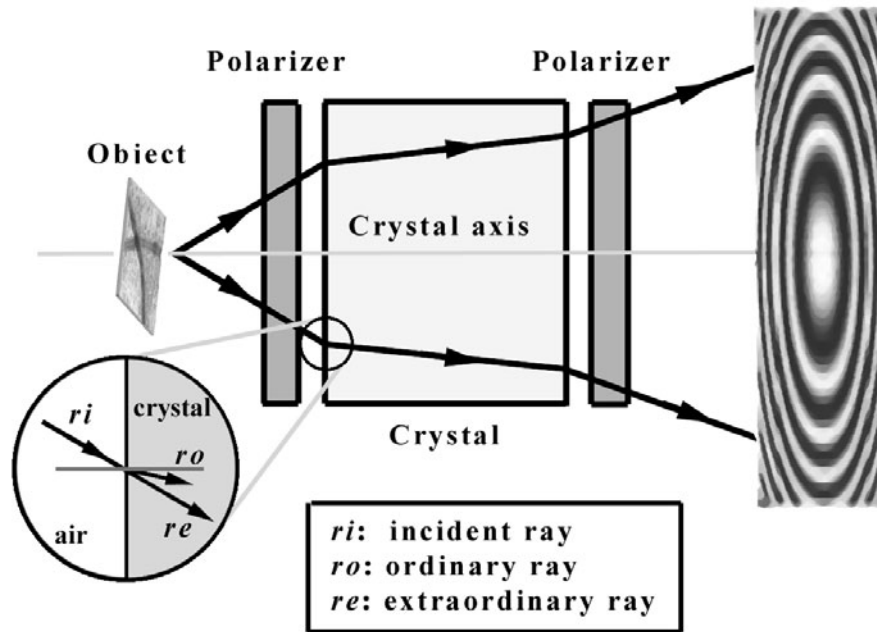


Figure 1 - Schirripa Spagnolo et al.

Figure 1 (Figure1.tif)

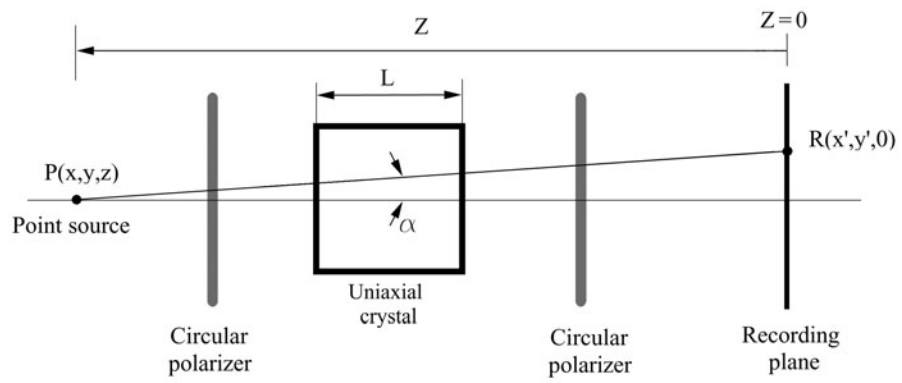


Figure 2 - Schirripa Spagnolo et al.

Figure 2 (Figure2.tif)

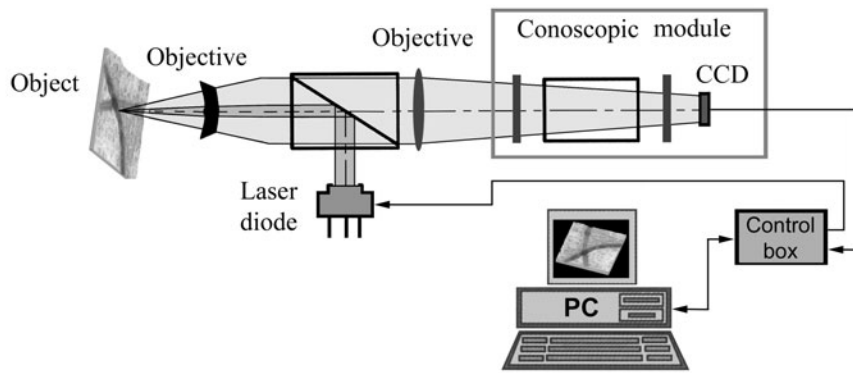


Figure 3 - Schirripa Spagnolo et al.

Figure 3 (Figure3.tif)

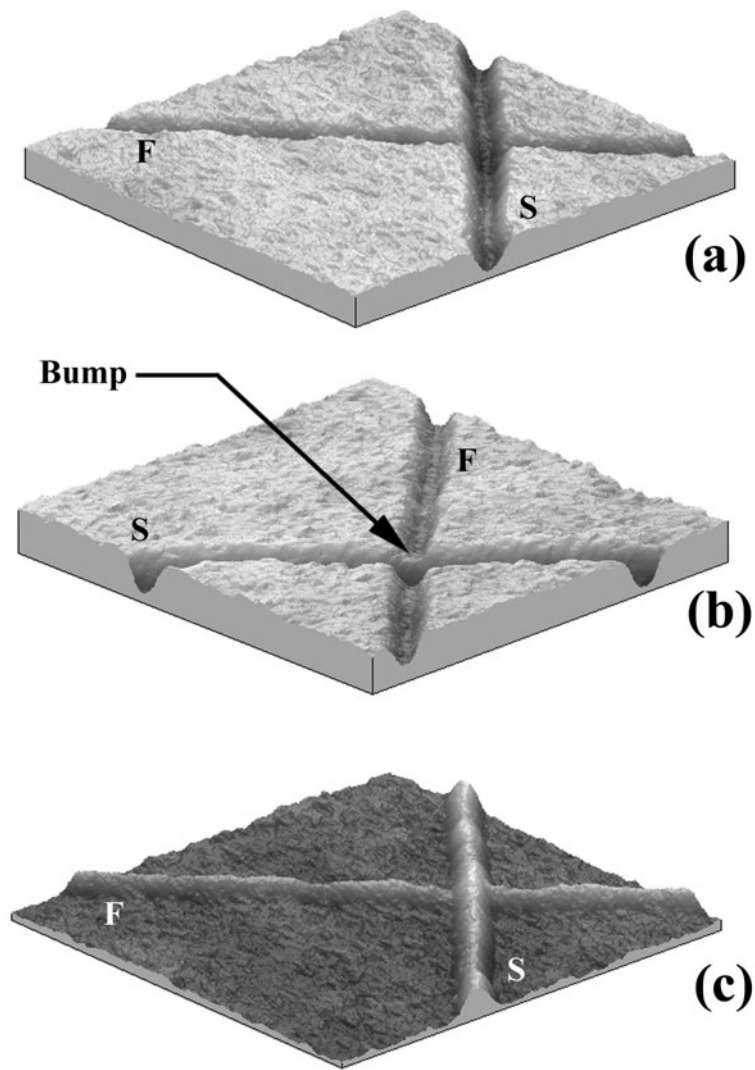


Figure 4 - Schirripa Spagnolo et al.

Figure 4 (figure 4.tif)

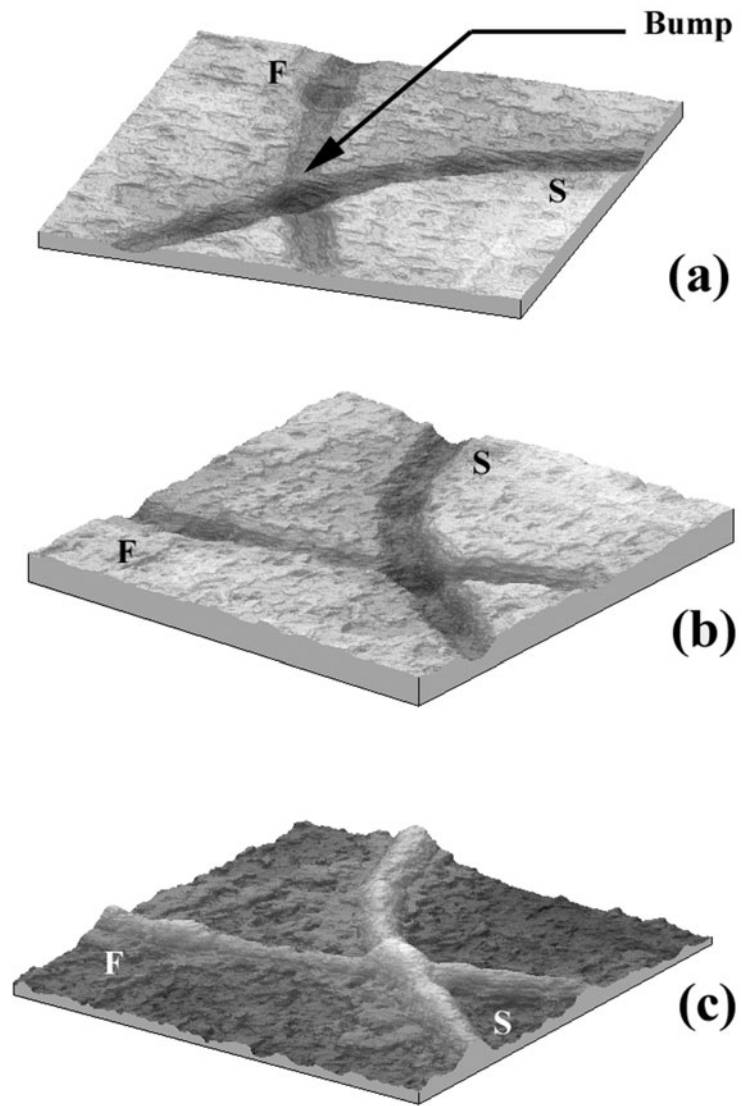


Figure 5 - G. Schirripa Spagnolo et al.

Figure 5 (figure5.tif)